Sample dependent response of a LaCl₃:Ce detector in prompt gamma neutron activation analysis of bulk hydrocarbon samples

A.A. Naqvi [a,*], Faris A. Al-Matouq [a], F.Z. Khiari [a], A.A. Isab [b], Khateeb-ur-Rehman [a], M. Raashid [a]

[a] Department of Physics, King Fahd University of Petroleum and Minerals, Dhahran, Saudi Arabia
[b] Department of Chemistry, King Fahd University of Petroleum and Minerals, Dhahran, Saudi Arabia

ARTICLE INFO

ABSTRACT

The response of a LaCl₃:Ce detector has been found to depend upon the hydrogen content of bulk samples in prompt gamma analysis using 14 MeV neutron inelastic scattering. The moderation of 14 MeV neutrons from hydrogen in the bulk sample produces thermal neutrons around the sample which ultimately excite chlorine capture gamma rays in the LaCl₃:Ce detector material. Interference of 6.11 MeV chlorine gamma rays from the detector itself with 6.13 MeV oxygen gamma rays from the bulk samples makes the intensity of the 6.13 MeV oxygen gamma ray peak relatively insensitive to variations in oxygen concentration. The strong dependence of the 1.95 MeV doublet chlorine gamma ray yield on hydrogen content of the bulk samples confirms fast neutron moderation from hydrogen in the bulk samples as a major source of production of thermal neutrons and chlorine gamma rays in the LaCl₃:Ce detector material.

Despite their poor oxygen detection capabilities, these detectors have nonetheless excellent detection capabilities for hydrogen and carbon in benzene, butyl alcohol, propanol, propanic acid, and formic acid bulk samples using 14 MeV neutron inelastic scattering.

1. Introduction

The application of Prompt Gamma Neutron Activation Analysis (PGNAA) technique is rapidly growing due to the utilization of radiation hardened lanthanum-halide (LaBr₃:Ce and LaCl₃:Ce) gamma ray detectors [1–11]. Although LaCl₃:Ce detectors [2–5] have comparable light output and energy resolution with LaBr₃:Ce detectors [6–11], they generate a higher background in thermal neutron fields due to thermal neutron capture in the chlorine of the LaCl₃:Ce detector material. Thermal neutrons are produced at the detector location due to moderation of 14 MeV neutrons from hydrogen in bulk samples. Therefore, chlorine background in LaCl₃:Ce detector in 14 MeV neutrons inelastic scattering studies is likely to increase with increasing hydrogen concentration. Consequently, the interference of chlorine capture gamma rays background from LaCl₃:Ce detector and gamma rays of interest from the bulk sample may limit the utilization of LaCl₃:Ce detectors in PGNAA applications.

The interference of 6.13 MeV prompt gamma rays of oxygen and 6.11 MeV chlorine capture gamma rays in LaCl₃:Ce detector material makes the oxygen concentration analysis in 14 MeV neutron inelastic scattering via 6.13 MeV peak intensity more complicated. For bulk samples with higher hydrogen concentrations, the oxygen full energy peak intensity is relatively insensitive to oxygen concentration variations in the samples.

KFUPM has acquired cylindrical 76 mm × 76 mm (height × diameter) LaBr₃:Ce [10,11] and LaCl₃:Ce [2] detectors for its environmental studies, concrete corrosion studies, explosive and contraband detection studies within its PGNAA program. Previously carbon, hydrogen and oxygen concentrations in bulk samples were measured in hydrocarbon samples in 14 MeV neutron inelastic scattering studies using a LaBr₃:Ce detector [10]. In the present study a LaCl₃:Ce detector has been used to measure hydrogen, carbon, and oxygen concentrations in the bulk hydrocarbon samples of benzene, butyl alcohol, propanol, propanic acid, and formic acid bulk samples using the 14 MeV neutrons-based PGNAA setup [10]. Hydrogen, carbon, and oxygen concentrations were measured using 2.22, 4.44 and 6.13 MeV prompt gamma rays, respectively. Interference of 6.13 MeV gamma rays from oxygen and 6.11 MeV gamma rays from chlorine in the LaCl₃:Ce detector material has been observed. Details of the present study are described in the following sections.

* Correspondence to: KFUPM Box 1815, Dhahran 31261, Saudi Arabia.
Tel.: +966 3860 4196; fax: +966 3860 2293.
E-mail address: aanaqvi@kfupm.edu.sa (A.A. Naqvi).

2. PGNAA of hydrocarbon samples using LaCl$_3$:Ce detector

The response of a LaCl$_3$:Ce detector was measured for high energy prompt gamma rays from hydrocarbon samples using the 14 MeV neutron-based PGNAA setup, described in detail elsewhere [10]. For continuity of text, the setup will be described briefly. It mainly consists of a cylindrical 90 mm140 mm (diameter × height) plastic container filled with the sample material and placed at 0° angle with respect to the neutron beam. The sample center is at a distance of 7.0 cm from the tritium target. The LaCl$_3$:Ce detector, placed at a center-to-center distance of 12.5 cm from the sample, views the sample at an angle of 90° with respect to the neutron beam axis. The detector is shielded against the neutrons and gamma rays by tungsten, paraffin and lead shielding, respectively. A pulsed beam of 14 MeV neutrons was produced via the T(d,n) reaction using a pulsed deuteron beam with 200 nano-sec width and a frequency of 31 kHz. A typical pulsed beam current of 60 μA was used. The fast neutron flux from the tritium target was monitored using a cylindrical 76 mm × 76 mm (diameter × height) NE213 fast neutron detector, placed at a distance of 1.8 m from the target and making an angle of 130° with respect to the beam. The prompt gamma-rays spectra of the LaCl$_3$:Ce detector were recorded for a preset time.

The elemental concentrations of the hydrocarbon bulk samples, as shown in Table 1, were independently verified using Atomic Absorption Spectrometry in the Department of Chemistry, King Fahd University of Petroleum and Minerals, Dhahran, Saudi Arabia. For prompt gamma ray analysis, the samples were prepared by filling the sample materials in the plastic containers. The containers were then irradiated in the PGNAA setup. The prompt gamma-ray data from the samples were acquired for 25 min using a Multichannel Buffer-based data acquisition system. The neutron flux spectrum, which was recorded during each run using the NE213 detector, was later used for neutron flux normalization during data correction. The NE213 detector was operated at half Cs-137 pulse height bias following the procedure described earlier [10].

2.1. PGNAA of water and benzene samples

Fig. 1(a) and (b) shows prompt gamma-rays pulse height spectra due to inelastic scattering of the neutrons from water and benzene samples superimposed upon each other. Water and benzene samples were chosen to show the effect of hydrogen contents of the bulk samples on the gamma ray response of the LaCl$_3$:Ce detector in 14 MeV neutron inelastic scattering studies. These samples represent extreme conditions i.e. the water sample does not contain carbon while the benzene sample does not contain oxygen but both samples contain 7 wt% and 11 wt% hydrogen, respectively. Fig. 1(a) shows the pulse height spectrum of gamma rays from benzene and water samples over 0.69–3.51 MeV energy showing lead gamma ray peaks at 1.06 and 2.62 MeV, produced due to inelastic scattering of the neutrons from lead shielding in the present study. This is consistent with previously reported results in the literature [13]. Gamma ray peak at 0.81 MeV is due to decay of ^{58}Co produced in 14 MeV neutron

Table 1
Elemental composition of the hydrocarbon samples.

Compound	Chemical formula	C (wt%)	H (wt%)	O (wt%)
Butyl alcohol	$C_6H_{10}O$	73.5	10.2	16.3
Propanol	C_3H_8O	60.0	13.3	26.7
Benzene	C_6H_6	92.3	7.7	0.0
Propanic acid	$C_3H_6O_2$	48.6	8.1	43.2
Formic acid	CH_2O_2	26.1	4.3	69.6
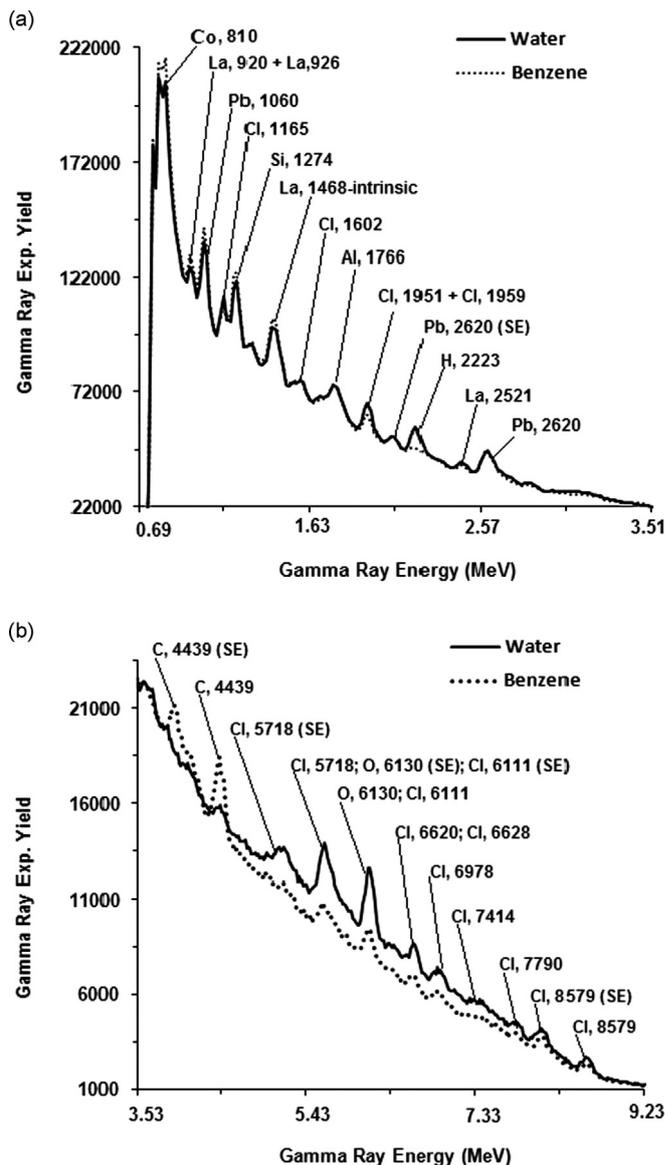
Fig. 1. Prompt gamma ray spectra of LaCl$_3$:Ce gamma ray detector from benzene, and water samples showing capture and inelastic scattering prompt gamma rays (a) over 0.68–3.51 MeV energy range and (b) over 3.53–9.23 MeV energy range.

induced ^{59}Co(n,2n) ^{58}Co reaction. Cobalt is found in many metal alloys used for magnets or beam lines. Fig. 1(a) also shows the single escape (SE) peak corresponding to the 2.62 MeV lead peak, 1.27 MeV silicon peak, the 1.77 MeV aluminum peak, along with the 0.92, 0.93, 1.47 (intrinsic activity) and the 2.52 MeV peaks from lanthanum. In Fig. 1(a) prompt gamma ray peaks due to thermal neutron capture in chlorine of LaCl$_3$:Ce material appear at 1.17, 1.60 and 1.95–1.96 MeV (later referred to as 1.95 MeV doublet). The intensities of 2.22 MeV hydrogen peak and 1.95 MeV chlorine peak are higher in the water spectrum than those in the benzene spectrum. The higher intensity of 1.95 MeV doublet chlorine gamma rays in the water sample as compared to the benzene sample is due to increasing thermalization of fast neutrons from higher hydrogen contents of the water sample. Therefore, the higher concentration of hydrogen in the water sample produces not only a higher intensity 2.22 MeV hydrogen capture gamma ray peak but also a higher intensity 1.95 MeV doublet chlorine capture peak in the LaCl$_3$:Ce spectrum.

This effect has been also observed in the higher energy part of the gamma ray spectra of water and benzene samples shown in

Table 2
Energies of prominent (n,n′γ) gamma-rays of oxygen [7] and chlorine [13].

	Gamma-ray energy (keV)	Reaction
O	2742	(n,n′γ)
	3089	(n,αγ)
	3684	(n,αγ)
	3854	(n,αγ)
	6130	(n,n′γ)
	6917	(n,n′γ)
	7117	(n,n′γ)
Cl	660	(n,n′γ)
	790	(n,n′γ)
	1210	(n,n′γ)
	1290	(n,n′γ)
	1780	(n,n′γ)
	2000	(n,n′γ)
	2150	(n,n′γ)
	2650	(n,n′γ)
	2710	(n,n′γ)
	3080	(n,n′γ)
	3170	(n,n′γ)
	3300	(n,n′γ)

Fig. 2. Enlarged LaCl₃:Ce detector prompt gamma ray spectra from the hydrocarbon samples plotted over 1.63–2.96 MeV energy range showing chlorine, lead and hydrogen capture peaks.

Fig. 3. Enlarged LaCl₃:Ce detector prompt gamma ray spectra from the hydrocarbon samples plotted over 3.53–4.86 MeV energy range showing carbon peaks.

Fig. 1(b) over 3.53–9.23 MeV. In the higher energy gamma ray spectra, chlorine peaks at 5.72, 6.11, 6.62–6.63 (later referred to as 6.62 MeV doublet), 6.98, 7.79 and 8.58 MeV are quite prominent. The intensity of these peaks is also higher for the water sample than for the benzene sample. The full energy and associated single escape peaks of oxygen 6.13 MeV gamma ray overlap with these peaks. Energies of prompt gamma rays produced due to inelastic scattering of 14 MeV neutrons from chlorine and oxygen are listed in Table 2. In the spectra of Fig. 1(b) the full energy peak of oxygen at 6.13 MeV contains a contribution from 6.11 MeV chlorine prompt gamma rays, whose intensity strongly depends upon the hydrogen content of the bulk samples. The 6.11 MeV chlorine prompt gamma rays full energy peak has a 6.6 barns cross-section [12]. The single escape peak of 6.13 MeV oxygen gamma ray contains contribution from both the overlapping 5.71 MeV full energy chlorine peak (with 1.8 barns cross-section [12]) and the single escape peak corresponding to 6.11 MeV chlorine peak. No such effects were observed in the prompt gamma spectra of hydrogen, carbon, and oxygen elements taken with a LaBr₃:Ce detector in a previous study [10].

2.2. PGNAA of the hydrocarbon bulk samples

Figs. 2–4 show the gamma ray pulse height spectra of the hydrocarbon samples, containing hydrogen, carbon and oxygen elemental concentrations over a broad range. Fig. 2 shows the enlarged pulse height spectra of the hydrocarbon bulk sample over 1.63–2.96 MeV energy range. The 2.22 MeV hydrogen and the 1.95 MeV doublet chlorine capture peaks are shown in Fig. 2 along with 2.6 MeV lead peak from lead shielding. The intensity of the hydrogen peak increases with hydrogen concentration with a maximum for propanol sample (13 wt% hydrogen concentration) and a minimum for the formic acid sample (4 wt% hydrogen concentration). Due to increasing flux of thermal neutrons with hydrogen concentration, the chlorine 1.95 MeV doublet peak intensity also increases with hydrogen concentration. The maximum intensity of the chlorine 1.95 MeV doublet peak has been observed for propanol while the minimum intensity has been observed for the formic acid, as expected.

In order to verify chlorine peak intensity dependence upon hydrogen concentration, the counts under the 1.95 MeV doublet chlorine peak in the hydrocarbon bulk samples were integrated and, after background subtraction and normalization, were plotted
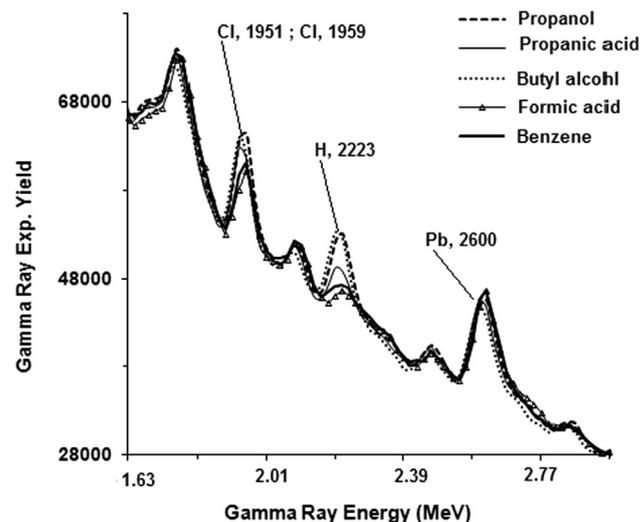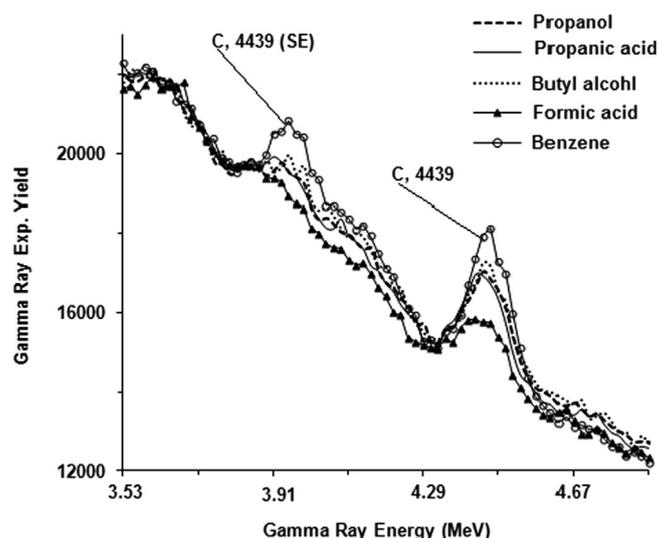
as a function of hydrogen concentration in the corresponding bulk samples.

Fig. 3 shows the enlarged pulse height spectra of the hydrocarbon bulk samples over 3.53–4.86 MeV energy range. It shows an increasing intensity of the 4.44 MeV carbon peak along with its associated single escape peak. Benzene and formic acid samples have the highest and the lowest peak intensities for 4.44 MeV carbon peaks, with 92 wt% and 26 wt% carbon concentrations, respectively. Fig. 4 shows the enlarged spectra of the hydrocarbon bulk samples over 4.86–7.14 MeV displaying the 5.72, 6.11, 6.62 MeV doublet, and 6.98 MeV chlorine peaks along with the 6.13 MeV oxygen peak. Also shown in Fig. 4 are the associated single escape (SE) peaks. Due to overlapping of 6.13 MeV oxygen and 6.11 MeV chlorine peaks and single escape peak of 6.62 MeV doublet chlorine peak, the resulting intensity of 6.13 MeV oxygen peak depends not only upon the oxygen, but also on the hydrogen contents of the bulk samples. Therefore a sample with high oxygen concentration and low hydrogen concentration has almost the same intensity of oxygen 6.13 MeV peak as compared to a sample with low oxygen concentration and high hydrogen concentration.
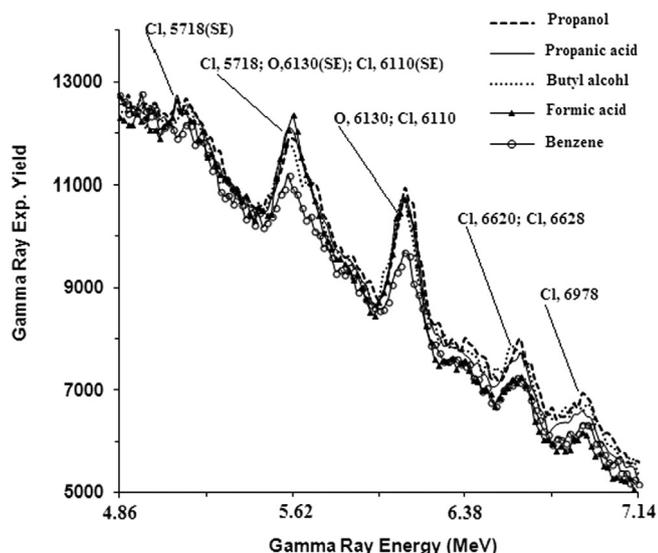
Fig. 4. Enlarged LaCl₃:Ce detector prompt gamma ray spectra from the hydrocarbon samples plotted over 4.86–7.14 MeV energy range showing oxygen and chlorine peaks.

However, our setup is sensitive to samples that are extremely deficient in O as shown in Fig. 4 for the case of benzene.

For hydrogen and carbon concentration analysis in the hydrocarbon bulk samples the hydrogen and carbon peak data in LaCl₃:Ce detector spectra were analyzed and the net counts under the hydrogen and carbon peaks were extracted by subtracting the container background spectra from the sample spectra. The net counts were then corrected for dead time and neutron flux variation using the procedure described earlier [10]. Finally, the gamma ray yield curves as a function of hydrogen and carbon concentrations in the bulk samples were generated. Figs. 5 and 6 show the gamma ray yields plotted as a function of hydrogen and carbon concentration, respectively, in the hydrocarbon samples. The solid lines in Figs. 5 and 6 represent results of hydrogen and carbon prompt gamma-ray calculated yields from the hydrocarbon samples obtained through Monte Carlo calculation using the MCNP4C code [14] following the procedure described elsewhere [10]. In Fig. 5, the integrated normalized experimental yield of chlorine 1.95 MeV doublet prompt gamma rays has also been superimposed on the integrated normalized yield of 2.22 MeV hydrogen peak yield. The solid line is a Monte Carlo fit to the experimental data. Within experimental uncertainties, chlorine and hydrogen peak data overlap each other. The excellent agreement between the theoretical and the experimental yields of hydrogen and carbon prompt gamma-rays as a function of their respective concentrations in the bulk samples shows the successful application of LaCl₃:Ce detector in hydrogen and carbon concentrations measurements in the hydrocarbon bulk samples.

Lastly, full energy (FE) and SE peaks of oxygen from the hydrocarbon samples were analyzed. In this analysis FE and SE peaks from the hydrocarbon samples were integrated and then benzene sample integrated counts were subtracted from the remaining samples as background (due to zero oxygen concentration). Fig. 7 shows benzene sample counts subtracted gamma ray yield plotted as a function of oxygen concentration in hydrocarbons samples. As expected FE peak yield is practically insensitive to oxygen concentration but SE peak yield shows a weak linear dependence of gamma ray yield on oxygen concentration due to small difference between various SE peaks heights of the hydrocarbon samples.

Finally the minimum detectable concentration, MDC, and its associated error, σ_{MDC}, were calculated for hydrogen and carbon in
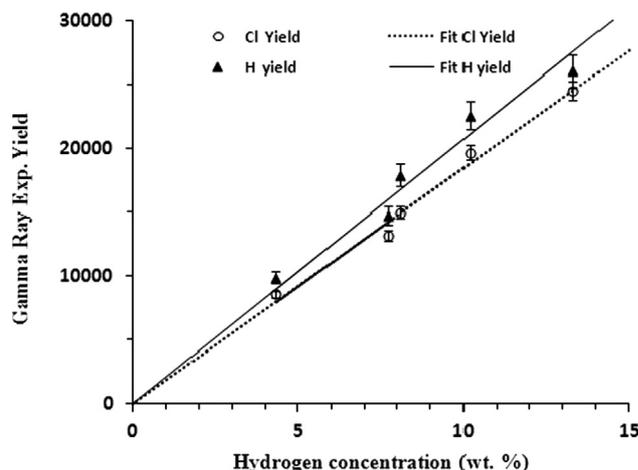
Fig. 5. Integrated normalized experimental yield of 2.22 MeV peak of hydrogen prompt gamma rays taken with the LaCl₃:Ce detector and integrated experimental yield of chlorine 1.95 MeV doublet prompt gamma rays, plotted as a function of hydrogen concentration in the hydrocarbon samples. The solid line is Monte Carlo fit to the experimental data.
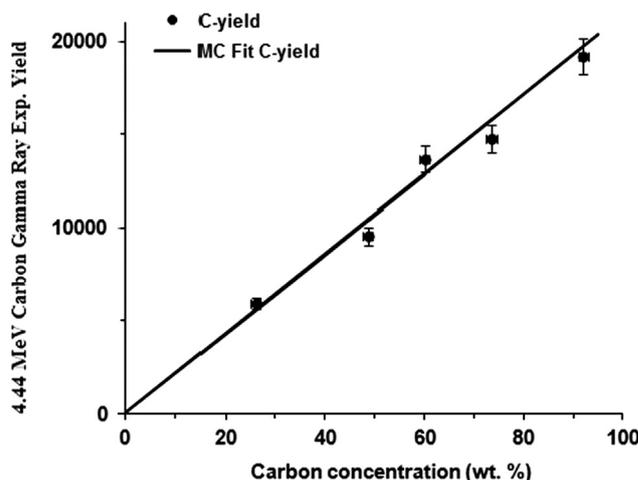
Fig. 6. Integrated normalized experimental yield of carbon 4.44 MeV prompt gamma rays taken with the LaCl₃:Ce detector, plotted as a function of carbon concentration in the hydrocarbon samples. The solid line is Monte Carlo fit to the experimental data.
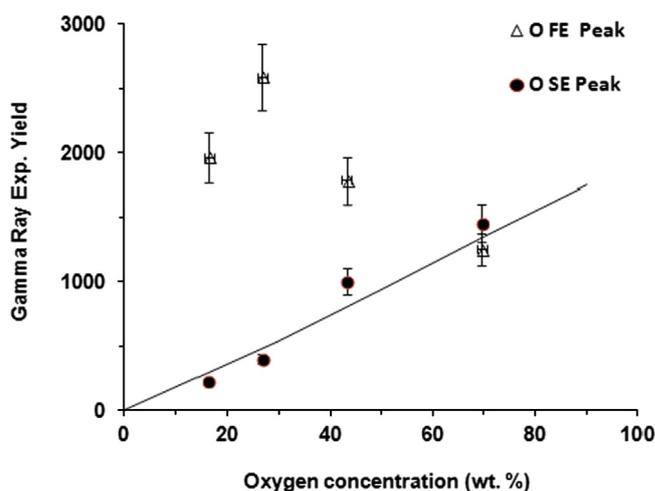
Fig. 7. Integrated normalized experimental yield of oxygen 6.13 MeV full energy (FE) and single escape (SE) prompt gamma rays taken with the LaCl₃:Ce detector, plotted as a function of carbon concentration in the hydrocarbon samples. The solid line is Monte Carlo fit to the experimental data.

Table 3
MDC of hydrogen, carbon and oxygen elements for 14 MeV neutron based PGNAA setup using LaCl$_3$:Ce (present study) and LaBr$_3$:Ce [10].

Detector	MDC$_H$ (wt%)	MDC$_C$ (wt%)	MDC$_O$ (wt%)
LaBr$_3$:Ce	0.5 ± 0.1	12.2 ± 3.8	15.8 ± 4.8
LaCl$_3$:Ce	1.11 ± 0.32*1.67 ± 0.51	9.68 ± 2.94	–

* MDC of hydrogen using 1.95 MeV doublet chlorine gamma rays.

the hydrocarbon samples, as described in Ref. [15]. The detection limit for an elemental concentration MDC measured under a peak with net counts P and associated background counts B (under the peak) can be approximated using the equation [16]

$$MDC = 3.29C\left\{ \sqrt{\left[\left(1+\frac{\eta_P}{\eta_B}\right)\right]} \Big/ \sqrt{\left[t'\left(\frac{P}{B}\right)\left(\frac{P}{t}\right)\right]} \right\}$$

where C is the element's concentration in the peak, t' is the counting time, P/t is net count rate, and η_P and η_B are the number of channels used to integrate the peak and background areas to calculate P and B counts. If η_P and η_B are equal and t' and t are equal then the equation reduces to:

$$MDC = 4.653\left(\frac{C}{P}\right)\sqrt{B}$$

where C/P is concentration (wt%)/counts, i.e. the calibration constant of the setup for a specific gamma ray peak. This is the Currie Equation of Minimum Detection Limit (MDL) of counts given by Knoll [17], with counts converted into element concentration.

The error in MDC i.e.

$$\sigma_{MDC} = \left(\frac{C}{P}\right)\sqrt{2B}$$

For 90 mm × 140 mm (diameter × height) cylindrical hydrocarbon bulk samples, the MDC of the KFUPM 14 MeV neutron-based PGNAA setup was calculated for hydrogen and carbon concentration measurement data taken with the LaCl$_3$:Ce detector using 2.22 MeV and 4.44 MeV gamma ray respectively. The MDC data for the LaCl$_3$:Ce detector are listed in Table 3. For comparison MDC of hydrogen calculated using 1.95 MeV chlorine peak is also included in Table 3. As expected from Fig. 7 MDC of hydrogen calculated using hydrogen peak agrees within statistical uncertainties with that calculated using the chlorine peak.

For the purpose of comparison, the MDC values for hydrogen, carbon and oxygen in bulk samples measured using a LaBr$_3$:Ce detector [10] have also been included in Table 3. Apparently values of MDC for carbon seems to be comparable for both the LaCl$_3$:Ce and the LaBr$_3$:Ce detectors, while for hydrogen MDC for the LaCl$_3$:Ce detector is two times poorer than that for the LaBr$_3$:Ce detector.

3. Conclusion

In 14 MeV neutron inelastic scattering studies, the response of a LaCl$_3$:Ce detector has been found to depend upon sample composition during the detection of H, C, and O elements prompt gamma rays from the hydrocarbon bulk samples. Interference of 6.11 MeV chlorine gamma rays from the LaCl$_3$:Ce detector has been observed with 6.13 MeV oxygen gamma rays from the bulk samples thereby making the oxygen peak intensity practically insensitive to oxygen concentration variations in the bulk samples. The yield of chlorine 1.95 MeV doublet prompt gamma rays from LaCl$_3$:Ce detector increases with hydrogen concentration in the samples, confirming neutron moderation effect in the bulk samples. In spite of the chlorine and the oxygen peak interference, the LaCl$_3$:Ce gamma ray detector has excellent efficiency for the measurement of hydrogen and carbon concentrations in bulk samples using the 14 MeV neutron-based PGNAA setup.

References

[1] D. Alexiev, L. Mo, D.A. Prokopovich, M.L. Smith, M. Matuchova, IEEE Transactions on Nuclear Sciences 55 (3) (2008) 1174.
[2] A.A. Naqvi, M.S. Al-Anezi, Zameer Kalakada, Faris A. Al Matouq, M. Maslehuddin, M.A. Gondal, A.A. Isab, Khateeb-ur-Rehman, M. Dastageer, Applied Radiation and Isotopes 70 (2012) 882.
[3] M. Balcerzyk, M. Moszyński, M. Kapusta, Nuclear Instruments and Methods in Physics Research A 537 (2005) 50.
[4] A. Owens, A.J.J. Bos, S. Brandenburg, C. Dathy, P. Dorenbos, S. Kraft, R.W. Ostendorf, V. Ouspenski, F. Quarati, Nuclear Instruments and Methods in Physics Research A 574 (2007) 110.
[5] K.S. Shah, J. Glodo, M. Klugerman, L. Cirignano, W.W. Moses, S.E. Derenzo, M.J. Weber, Nuclear Instruments and Methods in Physics Research A 505 (2003) 76.
[6] S. Davorin, S. Pesente, G. Nebbia, G. Viesti, V. Valkovic, Nuclear Instruments and Methods in Physics Research B 261 (2007) 321.
[7] C. Eleon, B. Perot, C. Carasco, D. Sudac, J. Obhodas, V. Valkovic, Nuclear Instruments and Methods in Physics Research A 629 (2011) 220.
[8] M. Ciema, D. Balabanski, M. Csatlo, J.M. Daugas, G. Georgiev, J. Gulya, M. Kmiecik, A. Krasznahorkay, S. Lalkovski, A. Lefebvre-Schuhl, R. Lozeva, A. Maj, A. Vitez, Nuclear Instruments and Methods in Physics Research A 608 (2009) 76.
[9] A. Favalli, H.C Mehner, V. Ciriello, B. Pedersen, Applied Radiation and Isotopes 68 (2010) 901.
[10] A.A Naqvi, Fares A. Al-Matouq, F.Z. Khiari, A.A. Isab, Khateeb-ur-Rehman, M. Raashid, Nuclear Instruments and Methods in Physics Research A 684 (2012) 82.
[11] A.A. Naqvi, Zameer Kalakada, M.S. Al-Anezi, M. Raashid, Khateeb-ur-Rehman, M. Maslehuddin, M.A. Garwan, F.Z. Khiari, A.A. Isab, O.S.B. Al-Amoudi, Nuclear Instruments and Methods in Physics Research A 665 (2011) 74.
[12] H.D. Choi, R.B. Firestone, R.M. Lindstrom, G.L. Molnár, S.F. Mughabghab, R. Paviotti-Corcuera, Z. Révay, A. Trkov, V. Zerkin, Chunmei Zhou, Database of prompt Gamma Rays from Slow Neutrons Capture for Elemental Analysis, IAEA, 2007, Available at: ⟨http://www.pub.iaea.org/MTCD/publications/PDF/Pub1263_web.pdf⟩.
[13] F.C. Engesser, W.E. Thompson, Journal of Nuclear Energy 21 (1967) 487.
[14] J.F. Briesmeister (Ed.), Los Alamos National Laboratory Report, 1997 LA-12625-M.
[15] A.A. Naqvi, M.M. Nagadi, O.S.B. Al-Amoudi, Nuclear Instruments and Methods in Physics Research A 569 (2006) 803.
[16] D.A. Gedcke, How Counting Statistics Controls Detection Limits and Peak Precession, ORTEC Application Notes AN59, Available from: ⟨www.ortec-online.com⟩.
[17] G.F. Knoll, Radiation Detection and Measurements, John Wiley, 2000.